研究成果の刊行に関する一覧表

雑誌

発表者氏名	論文タイトル名	発表誌名	巻号	ページ	出版年
Katano H, Hogaboam CM	Herpes virus-associated pulmonary hypertension.	Am J Resp Crit Care Med	172	1485-1486	2005
Satoh M, Kaneko A, Kokaze A, Katano H, Sata T	Seroprevalence of Human Herpesvirus 8 on Vanuatu islands in eastern Melanesia.	Jpn J Infect Dis	59	63-65	2006
Asahi-Ozaki Y, Sato Y, Kanno T, Sata T, Katano H	Quantitative analysis of Kaposi's sarcoma-associated herpesvirus (KSHV) in KSHV-associated diseases.	J Infect Dis	193	773-782	2006
Hishima T, Oyaizu N, Fujii T, Tachikawa N, Ajisawa A, Negishi M, Nakamura T, Iwamoto A, Hayashi Y, Matsubara D, Sasao Y, Kimura S, Kikuchi Y, Teruya K, Yasuoka A, Oka S, Saito K, Mori S, Funata N, Sata T, Katano H	Decrease of Epstein-Barr virus-positive AIDS-related lymphoma in the era of highly active antiretroviral therapy.	Microbes Infect		In press	2006

MAJOR ARTICLE

Quantitative Analysis of Kaposi Sarcoma–Associated Herpesvirus (KSHV) in KSHV-Associated Diseases

Yasuko Asahi-Ozaki, Yuko Sato, Takayuki Kanno, Tetsutaro Sata, and Harutaka Katano

Department of Pathology, National Institute of Infectious Diseases, Shinjuku, Tokyo, Japan

Background. Accurate numbers of copies of Kaposi sarcoma–associated herpesvirus (KSHV) and numbers of virus-infected cells in lesions caused by KSHV-associated diseases are unknown.

Methods. Quantitative polymerase chain reaction (PCR) and computerized imaging of immunohistochemical analysis were performed on pathologic sections of samples from persons with KSHV-associated diseases.

Results. Real-time PCR and semiquantitative PCR–Southern blotting demonstrated that DNA extracted from biopsy samples of KS lesions contained ~1–2 viral copies/cell. KSHV-associated lymphoma contained 10–50 viral copies/cell. Computerized-image analysis demonstrated that ~49% of cells expressed KSHV-encoded latency-associated nuclear antigen in KS biopsy samples. On the basis of results of real-time PCR and computerized-image analysis, the predicted number of viral copies was 3.2 viral copies/cell in KS lesions. Computerized-image analysis also revealed that the expression of open-reading frame (ORF)–50 protein, an immediate early protein of KSHV, was very rare in KS lesions, which implies that they were mainly composed of proliferating cells latently infected with KSHV. In multicentric Castleman disease lesions, 25% of virus-infected cells expressed ORF50 protein, which suggests the frequent lytic replication of KSHV.

Conclusions. Numbers of viral copies and of virus-positive cells vary among KSHV-associated diseases, which suggests different mechanisms of viral pathogenesis. The combination of real-time PCR and computerized-image analysis provides a useful tool for the assessment of the number of viral copies in KSHV-associated diseases.

Kaposi sarcoma–associated herpesvirus (KSHV, also called human herpesvirus [HHV]–8) has been detected by polymerase chain reaction (PCR) and immunohistochemical analysis in almost all cases of KS, regardless of HIV infection status [1–6]. Primary effusion lymphoma (PEL) is also a KSHV-associated disease [7], and KSHV-associated solid lymphoma has been reported to be a variant of PEL that forms solid tumors [8, 9]. Some, but not all, cases of multicentric Castleman disease (MCD) are also KSHV positive [10, 11].

Similarly to other herpesviruses, KSHV has 2 phases of infection: lytic and latent [1, 12]. During the lytic phase, KSHV replicates in infected cells, which results in cell lysis. However, the virus does not replicate in latently infected cells, although they harbor viral episomes and express several KSHV-encoded latency-associated proteins, such as latency-associated nuclear antigen (LANA) and LANA2 [1, 13, 14]. Although latent infection predominates in KSHV-infected PEL cell lines, phorbol ester stimulation can induce lytic infection in these cells [12]. Gene expression during the lytic phase is classified into immediate early, early, and late expression [12]. Open-reading frame (ORF)–50 was identified as an immediate early protein that was required for the lytic replication of KSHV [12, 15, 16]. Immunohistochemical studies demonstrated that KS cells expressed LANA; however, the expression of lytic proteins was very rare in KS lesions, which suggests that latent infection predominates in KS cells [5, 6, 17]. Lytic proteins are expressed by some B cells in the mantle zone of MCD, which suggests that lytic replication frequently occurs in MCD lesions [6, 17].

Numbers of KSHV copies in KSHV-associated diseases have been investigated by several groups [18–26]. An early study that used conventional PCR and South-

Received 10 August 2005; accepted 28 September 2005; electronically published 7 February 2006.

Financial support: Ministry of Health, Labor and Welfare (Health and Labor Sciences Research Grants on HIV/AIDS and Measures for Intractable Diseases H15-AIDS-005 to H.K. and 17243601 to T.S.); Ministry of Education, Culture, Sports, Science and Technology of Japan (Grant-in-Aid for Scientific Research 17590365 to H.K.); Japan Health Sciences Foundation (research grant on health sciences focusing on drug innovation SA14831 to H.K.).

Potential conflicts of interest: none reported.

Reprints or correspondence: Dr. Harutaka Katano, Dept. of Pathology, National Institute of Infectious Diseases, 1-23-1 Toyama, Shinjuku, Tokyo 162-8640, Japan (katano@nih.go.jp).

The Journal of Infectious Diseases 2006;193:000–000

0022-1899/2006/19306-00XX$15.00

Table 1. No. of copies of Kaposi sarcoma–associated herpesvirus (KSHV), determined by real-time polymerase chain reaction (PCR) and PCR–Southern blot.

	Real-time PCR		PCR–Southern blot	
Patient (disease)	Mean copies/cell	Average (SD)	No.	Mean copies/cell
1 (PEL)	82.01	82.01	1	50
2 (KSHV-associated solid lymphoma)	14.26	10.75 (4.97)	...	...
3 (KSHV-associated solid lymphoma)	7.23		2	2
4 (AIDS-associated patch KS)	0.09	0.13 (0.11)	...	...
5 (AIDS-associated plaque KS)	0.04		...	...
6 (AIDS-associated patch KS)	0.25		...	...
7 (AIDS-associated nodular KS)	0.67	1.72 (1.51)	3	2
8 (AIDS-associated nodular KS)	1.02		4	0.4
9 (AIDS-associated nodular KS)	0.53		...	...
10 (AIDS-associated nodular KS)	3.13		5	0.4
11 (AIDS-associated nodular KS)	3.93		6	2
12 (AIDS-associated nodular KS)	0.14		...	...
13 (AIDS-associated nodular KS)	3.41		...	...
14 (AIDS-associated nodular KS)	0.91		...	...
15 (classic patch KS)	0.16	2.60 (2.70)	...	...
16 (classic patch KS)	5.50		7	0.08
17 (classic patch KS)	2.13		...	...
18 (classic nodular KS)	0.00	1.64 (2.63)	...	...
19 (classic nodular KS)	4.67		8	2
20 (classic nodular KS)	0.25		...	...
21 (MCD)	0.27	0.27	9	1
22 (control, BCBL-1)	78.01	87.08 (12.83)	...	...
23 (control, TY-1)	96.15		...	...

NOTE. MCD, multicentric Castleman disease; PEL, primary effusion lymphoma.

ern blot analysis demonstrated that a PEL cell contained ~50 copies of KSHV genome, whereas the KSHV genome was detected at a rate of ~1 viral copy/cell in KS lesions [18]. Recently, real-time PCR was used to detect KSHV, and several reports have described numbers of viral copies in peripheral blood mononuclear cells (PBMCs) derived from patients with KS [19–26]. Studies using real-time PCR have demonstrated that numbers of viral copies in PBMCs varied among diseases and disease stages [21–24]. However, to our knowledge, there has been no report that has compared numbers of viral copies in KS, PEL, or MCD lesions using real-time PCR. Therefore, the aim of the present study was to determine numbers of viral copies in lesions of KSHV-associated diseases using pathologic samples. Pathologic tissue samples—such as biopsy samples—frequently contain both virus-infected cells and noninfected cells. Thus, results from real-time PCR do not solely represent numbers of viral copies in virus-infected cells. To solve this problem, we combined real-time PCR with computerized-image analysis that allowed an assessment of numbers of virus-infected cells in immunostained sections. Using these methods, we identified numbers of both viral copies and virus-infected cells in appropriate sections. Thus, we obtained relatively accurate numbers of viral copies in histologic sections of KSHV-associated disease lesions.

PATIENTS, MATERIALS, AND METHODS

Patients and samples. All patients provided informed consent for specimens to be obtained. For PCR analysis, 21 clinical samples were collected (table 1). For immunohistochemical analysis, 27 histopathologic specimens from KSHV-infected patients (table 2) were collected from 1995 to 2004. All KS specimens were categorized into groups according to the clinical stage of KS (patch, plaque, or nodular) on the basis of clinical and histologic data. DNA extracted from 2 KSHV-positive cell lines (BCBL-1 and TY-1), a KSHV-negative Epstein-Barr virus–positive Burkitt lymphoma cell line (Raji), and human umbilical vascular endothelial cells (HUVECs) was used as a control for PCR studies [27, 28].

Preparation of DNA. DNA was extracted from fresh-frozen clinical materials or from formalin-fixed, paraffin-embedded tissue samples from 21 biopsies of KSHV-infected patients (table 1). For fresh-frozen materials, the DNeasy Tissue Kit (Qiagen) was used in accordance with the manufacturer's instructions. For the isolation of DNA from formalin-fixed, paraffin-embedded biopsy samples, 5-μm sections (n = 3–4) were deparaffinized with xylene, digested with proteinase K, and processed for phenol/chloroform extraction with sodium acetate/ethanol precipitation.

Table 2. Percentage of latency-associated nuclear antigen (LANA)– or open-reading frame (ORF)–50–positive cells in immunohistochemical analysis (IHC) with computerized-image analysis.

IHC, samples	Cases, no.	Minimum/maximum (average), %
LANA		
AIDS-associated patch/plaque KS	11	12/95 (48)
AIDS-associated nodular KS	4	28/72 (57)
AIDS-associated KS involving LN	2	28/31 (30)
AIDS-associated KS involving GI tract	2	6/7 (7)
Classic patch/plaque KS	2	25/47 (36)
MCD	4	5/21 (8)
KSHV-associated solid lymphoma	2	79/80 (80)
ORF50		
AIDS-associated patch/plaque KS	5	0
AIDS-associated nodular KS	4	0
Classic KS, patch/plaque	2	0
MCD	5	1/3 (2)
KSHV-associated solid lymphoma	2	0/5 (3)

NOTE. GI, gastrointestinal; KSHV, Kaposi sarcoma–associated herpesvirus; LN, lymph node; MCD, multicentric Castleman disease.

Real-time quantitative PCR. Amounts of KSHV DNA were determined by quantitative real-time (TaqMan) PCR using the ABI Prism 7900HT sequence detection system (Applied Biosystems), which amplified segments within the KSHV LANA gene (one of the latent proteins coded on ORF73). Sequences and usage parameters of primers and probes have been described elsewhere [19]. We also determined the amounts of human genomic DNA that were present in DNA extracted from each specimen. Primers and probes for the gene encoding human glyceraldehyde 3-phosphate dehydrogenase (GAPDH) were designed, using Primer Express software (Applied Biosystems), to obtain a 104-bp amplicon. Forward and reverse primer sequences were 5′-GCTCCCTCTTTCTTTGCAGCAAT-3′ and 5′-TACCATGAGTCCTTCCACGATAC-3′, respectively. The fluorogenic TaqMan probe was 5′-(FAM)TCCTGCACCACCAACTGCTTAGCACC(TAMRA)-3′. PCR amplification was performed in 25-μL reaction mixtures using QuantiTect probe PCR Master Mix (Qiagen), 0.4 μmol/L each primer, 0.2 μmol/L TaqMan probe, and 2 μL of isolated DNA. PCR conditions were 15 min at 95°C, followed by 45 cycles of 15 s at 94°C and 1 min at 60°C. Quantitative results were obtained by generating standard curves for pGEM-T plasmids (Promega) that contained each KSHV (ORF73) and cellular target (GAPDH) amplicon. The number of viral copies per cell was calculated by dividing the number of ORF73 copies by one-half of the number of GAPDH copies, because there are 2 alleles of GAPDH in each cell.

Detection of KSHV by semiquantitative PCR–Southern blotting analysis. Semiquantitative PCR–Southern blotting was performed to determine copy numbers of KSHV in DNA samples after PCR amplification of $KS330_{233}$ [11, 29]. The β-globin gene was simultaneously amplified as described elsewhere [11]. For PCR–Southern blot analysis, digoxygenin (DIG)–labeled $KS330_{233}$ and a 110-bp DNA fragment of the β-globin gene, whose sequences were confirmed by sequencing, were used as probes [11]. Procedures for Southern blot analysis and the detection of DIG were those of the manufacturer (Roche Diagnostic). Copy numbers of KSHV were determined by comparing results for $KS330_{233}$ and β-globin, on the basis of the information that each cell has 2 copies of the β-globin genome.

Histologic and immunohistochemical analyses. Serial sections were prepared and stained with hematoxylin-eosin (HE) for light microscopy or were subjected to immunohistochemical staining with antiserum against LANA or ORF50 proteins (lytic antigens) [4, 30]. Immunohistochemical staining was visualized using the avidin-streptavidin-peroxidase method with 3-3′diaminobenzidine as the chromogen, as described elsewhere [4, 30]. For double immunohistochemical staining of vascular endothelial cell growth factor receptor–3 (VEGFR-3) and LANA, an anti-LANA rabbit polyclonal antibody, a peroxidase-conjugated anti-rabbit goat antibody (Envision; Dako Cytomation), and aminoethylcarbazole (AEC; Nichirei) were used as the primary antibody, secondary antibody, and chromogen, respectively. After the color development of AEC, slides were washed with PBS and processed for VEGFR-3 staining. Anti–VEGFR-3 mouse monoclonal antibody (D2-40; Nichirei) and alkaline phosphatase–conjugated anti–mouse IgG goat antibody (Envision; Dako Cytomation) were used, and a positive signal was detected with Fast Blue BB (Sigma-Aldrich). Slides were mounted with a glycerol-based mounting solution.

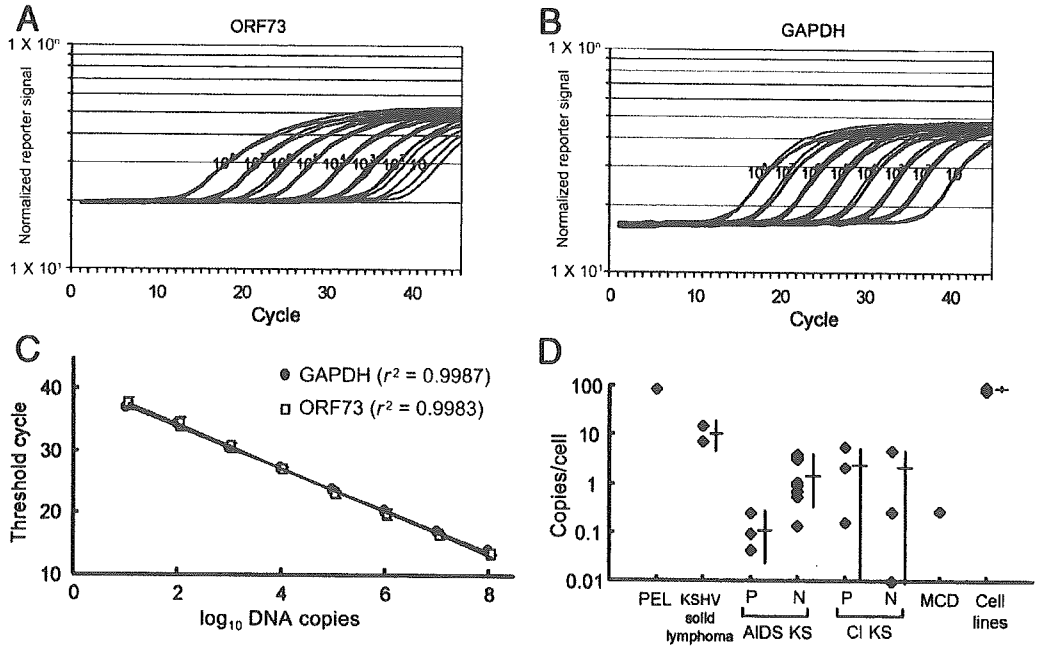

Figure 1. No. of copies of Kaposi sarcoma–associated herpesvirus (KSHV) in KSHV-associated diseases, determined by real-time polymerase chain reaction (PCR). *A* and *B*, Amplification curves of open-reading frame (ORF)–73 *(A)* and glyceraldehyde 3-phosphate dehydrogenase (GAPDH) genomes *(B)*. *C*, Standard curve of ORF73 and GAPDH genomes. *D*, No. of copies of KSHV per cell, calculated on the basis of the results of real-time PCR. Horizontal and vertical bars beside blots indicate average and SD, respectively. AIDS KS, AIDS-associated KS; Cl KS, classic KS; MCD, multicentric Castleman disease; N, nodular; P, patch; PEL, primary effusion lymphoma; Rn, normalized reporter signal.

Computerized-image analysis for KSHV-positive cells. To estimate numbers of KSHV-infected cells in lesions of KSHV-associated diseases, computerized analysis of immunohistochemical images was performed using ImageJ software (version 1.33u; National Institutes of Health). A representative image of each section from each sample was captured at ×40 or ×100 magnification. First, the image was split into red, green, and blue colors; then the 3 images were converted to gray-scale images. The total number of cells was counted in the red image, and the number of KSHV-infected cells (stained by the antiserum against KSHV proteins) was counted in the blue image. A threshold was set, for clear visualization of the displayed image. For counting cells, "analyze particle" was selected from "analyze" in the menu bar, and the minimum size was set at 30. After the accuracy of cell outlines generated by the software was verified, numbers of cells were calculated in separate windows.

RESULTS

Amount of KSHV viral genome in KSHV-associated lesions. To determine the relationships between amounts of KSHV genome and KSHV-associated diseases, we performed real-time PCR to detect KSHV ORF73 and GAPDH in appropriate DNA samples. Specificity of the assay for ORF73 was confirmed using a panel of DNA from other herpesviruses (HHV-1–7) and cellular DNA from HUVECs and Raji cells (data not shown). The assay for ORF73 uniformly detected 10 copies of pGEM-ORF73 plasmid (figure 1*A* and 1*C*). PCR amplification of GAPDH also uniformly detected 10 copies of GAPDH genome (figure 1*B* and 1*C*). Amplification plots and standard curves demonstrated a linear relationship between numbers of copies from 10 to 10^8 and the cycle threshold, which indicates that dynamic ranges of these 2 real-time PCRs were between 10 and 10^8 copies. To validate differences between DNA samples from frozen tissues and those from paraffin-embedded tissues, we tested a DNA sample from a frozen cell pellet of TY-1 and a DNA sample from a paraffin-embedded TY-1 cell pellet. No significant difference was detected between these 2 types of DNA (data not shown).

Results of real-time PCR showed signs of a positive association between the number of viral copies per cell and disease (table 1 and figure 1*D*). A DNA sample from PEL demonstrated a number of KSHV copies similar to that of PEL cell lines (PEL, 82; PEL cell lines, 87). DNA from samples of KSHV-associated solid lymphoma also showed a high number of KSHV copies (average, 10.8 viral copies/cell). DNA from samples of KS and MCD demonstrated lower numbers of viral copies than those of KSHV-associated lymphoma (PEL and KSHV-associated solid lymphoma). The average number of KSHV copies in DNA from KS samples was 1.58 viral copies/cell (range, 0.00–5.50

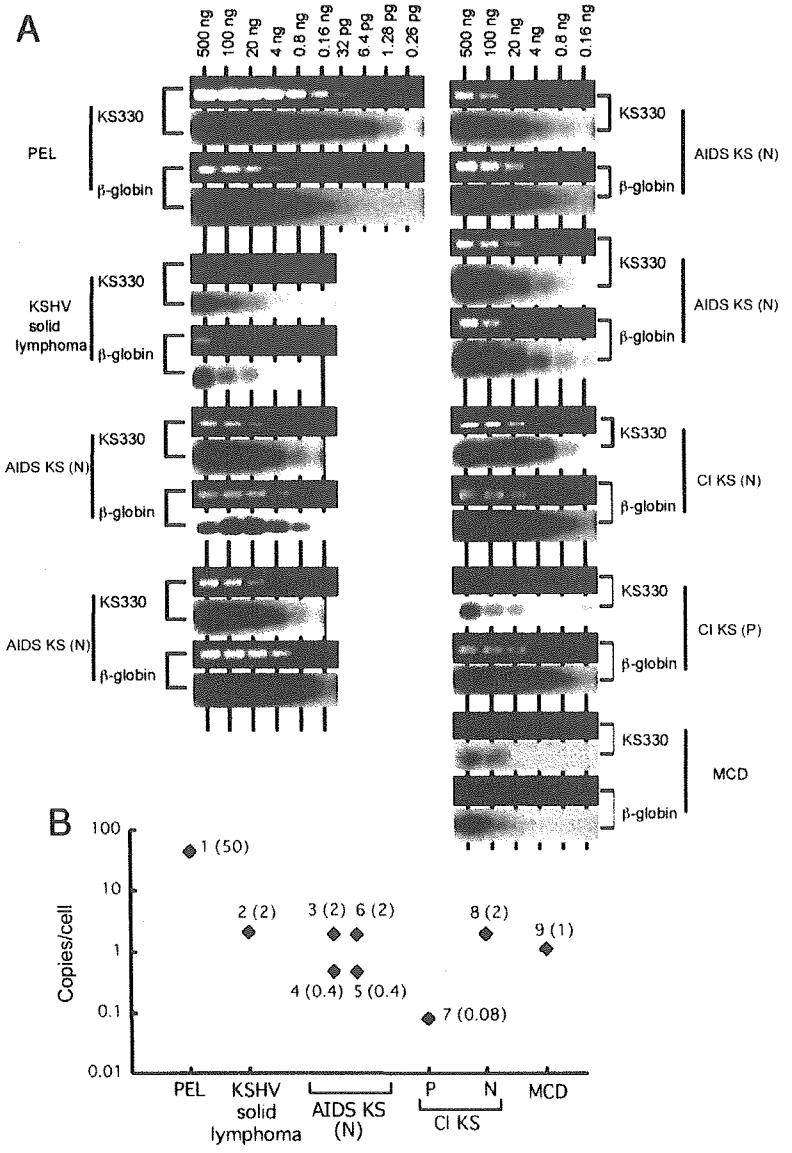

Figure 2. No. of copies of Kaposi sarcoma–associated herpesvirus (KSHV) in KSHV-associated disease, determined by conventional polymerase chain reaction (PCR)–Southern blotting. *A*, PCR–Southern blotting. DNA extracted from samples was serially diluted, and KS330 and β-globin genes were amplified from the diluted DNA. *Upper panels*, bands of PCR products in ethidium bromide–stained gel; *lower panels*, bands of products in PCR–Southern blots. *B*, No. of copies of KSHV in KSHV-associated diseases, determined by PCR–Southern blots. The nos. beside each dot correspond to the sample nos. in panel A. The nos. in parentheses indicate the nos. of viral copies per cell. AIDS KS, AIDS-associated KS; CI KS, classic KS; MCD, multicentric Castleman disease; N, nodular; P, patch.

viral copies/cell), whereas those in DNA samples from the nodular and patch/plaque stages of AIDS-associated KS samples were 1.72 and 0.13 viral copies/cell, respectively. DNA samples from classic KS (KS in patients without HIV infection) also had <5 viral copies/cell. A DNA sample from an MCD lesion had 0.27 viral copies/cell. To confirm these results, we performed semiquantitative PCR–Southern blot analysis using some of these samples. Results demonstrated similar copy numbers resulting from the 2 techniques (table 1 and figure 2). Thus, quantitative PCR analysis suggested that PEL might have the highest copy number (82 copies), followed by KSHV-associated solid lymphoma (11 copies). KS and MCD lesions contained lower copy numbers (~1 copy/cell), regardless of HIV-infection.

Number of KSHV-infected cells in KSHV-associated diseases. Because pathologic tissue samples present cells contaminated

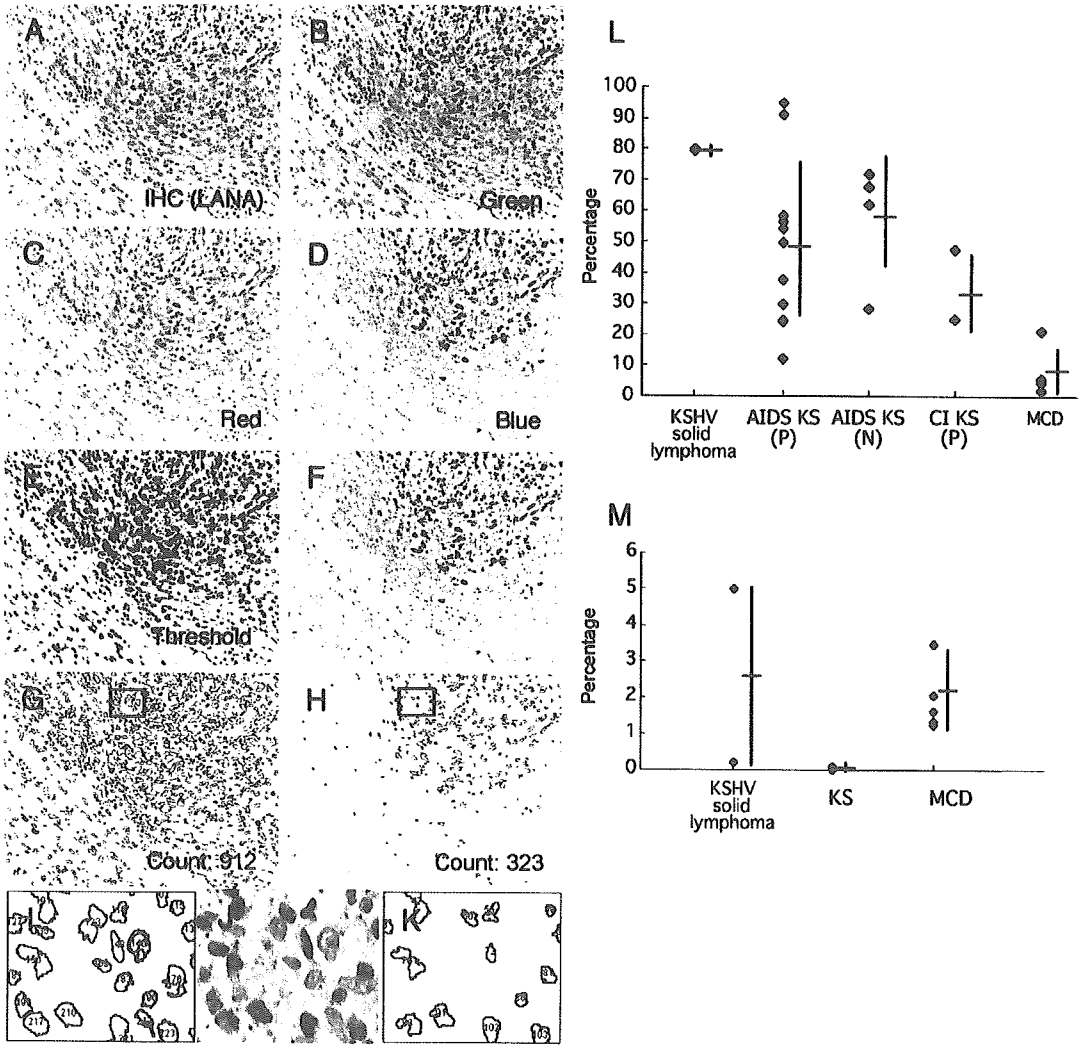

Figure 3. Computerized-image analysis of immunostaining. *A–K,* Samples of computerized-image analysis. *A,* Image of immunohistochemical analysis for latency-associated nuclear antigen (LANA) on the lymph node that Kaposi sarcoma (KS) cells infiltrate. *B–D,* Image separated in into red *(C),* green *(B),* and blue *(D)* splits. *E,* The threshold of all cells, determined on the basis of a red split. *F,* The threshold of positive cells, determined on the basis of a blue split. *G,* Tracing image of all cells. *H,* Tracing image of only positive cells. *I,* Enlarged image of a box from panel G. All cells were traced and counted. *J,* The image of immunohistochemical analysis corresponding to that in panel I. *K,* Enlarged image of a box in panel H. Only positive cells were traced and counted. *L,* Rate of LANA-positive cells in samples. Horizontal and vertical bars beside blots indicate the average and SD, respectively. *M,* Positive rate of open-reading frame (ORF)–50–positive cells. AIDS KS, AIDS-associated KS; CI KS, classic KS; KSHV, KS-associated herpesvirus; MCD, multicentric Castleman disease; N, nodular; P, patchy.

in varying degrees, all DNA samples that we used for real-time PCR actually contained DNA extracted from histologically normal cells and noninfected (LANA-negative) cells, as confirmed by histologic data. To determine accurate KSHV copy numbers in a KSHV-infected cell in a lesion, knowledge is required of accurate numbers of KSHV-infected cells in a specific sample. Thus, we performed computerized-image analysis of immunostained sections to estimate the number of KSHV-positive cells. Because it is recognized that all KSHV-infected cells express LANA in the nuclei, we counted cells expressing LANA in the nuclei as KSHV-infected cells. LANA was stained brown in immunohistochemical analysis, and cell nuclei were counterstained with hematoxylin (violet). Therefore, brown nuclei were counted as LANA-positive cells, and violet entities were counted as nuclei by the image-analysis software ImageJ (figure 3). Results revealed that 80% of cells in tissue samples from KSHV-associated solid lymphoma were LANA positive (table 2 and figure 3*L*). Tissues obtained from AIDS-associated and non–AIDS-associated KS contained 12%–95% (average, 49%) LANA-positive cells. The MCD sample contained 8% (range,

Table 3. No. of viral copies and percentage of latency-associated nuclear antigen (LANA–) or open-reading frame (ORF)–50–positive cells in Kaposi sarcoma–associated herpesvirus (KSHV)–associated diseases.

Samples	Detected viral copies/cell[a]	LANA positive,[b] %	ORF50 positive,[b] %	Lytic cells/ infected cells, %	Predicted viral copies/infected cell
PEL	82.01	ND	ND	ND	...
KSHV-associated solid lymphoma	10.7	80	3	4	13.4
KS	1.58	49	0	0	3.22
AIDS-associated KS	1.28	51	0	0	2.50
Patch/plaque	0.13	48	0	0	0.27
Nodular	1.72	57	0	0	3.02
Classic KS	2.12	36	0	0	5.89
MCD	0.27	8	2	25	3.38

NOTE. MCD, multicentric Castleman disease; ND, not done; PEL, primary effusion lymphoma.

[a] TaqMan polymerase chain reaction.

[b] Immunohistochemical analysis.

5%–21%) LANA-positive cells. By comparing results from quantitative PCR and computerized-image analysis, we predicted numbers of KSHV copies in virus-infected cells from KSHV-associated disease samples (table 3). The predicted number of KSHV copies was 3.2 viral copies/cell in KS lesions. We also counted cells positive for ORF50 protein, a lytic antigen encoded by KSHV (table 2 and figure 3*M*). There were 3% ORF50 protein–positive cells in KSHV solid lymphoma samples and even a smaller percentage in KS lesions (table 2 and figure 4). When we compared numbers of cells expressing ORF50 protein and those expressing LANA, it was clear that KS cells expressed LANA, but the expression of ORF50 protein was very rare in KS lesions (table 3). In MCD lesions, 2% of cells expressed ORF50 protein. Although only 8% of cells were virus infected in MCD lesions, 25% of virus-infected cells expressed ORF50 protein, which suggests the frequent lytic replication of KSHV in MCD. These data demonstrated that number of viral copies and positivity for LANA varied among KSHV-associated diseases, which suggests different mechanisms of viral pathogenesis.

Numbers of KSHV copies at each KS stage. KS lesions were categorized into 3 clinical stages: patch, plaque, and nodular. To determine the relationship between amounts of KSHV genome and KS clinical stage, amounts of viral genome and cellular gene present in DNA extracts from specimens at each KS stage were examined using quantitative real-time PCR (figure 1) and semiquantitative PCR–Southern blotting (figure 2). The number of KSHV copies was significantly lower in patch/plaque-stage lesions (range, 0.04–0.30 viral copies/cell; average, 0.13 viral copies/cell) than in nodular-stage lesions (range, 0.10–3.90 viral copies/cell; average, 1.72 viral copies/cell) ($P < .05$, Mann-Whitney *U* test). In contrast, the number of KSHV copies was similar in both patch/plaque- and nodular-stage lesions in classic KS. Computerized-image analysis of immunohistochemically stained sections revealed that LANA-positive cell populations in the nodular stage (57%) were larger than those in the patch/plaque stage (48%); however, there was no significant difference between them. Lytic ORF50 protein–positive cells were very rare (0%) in both stages (figure 3*L* and 3*M* and table 3), which implies that lesions in KS were mainly composed of proliferating KSHV latently infected cells. Differences in numbers of viral copies between the 2 stages in AIDS-associated KS may simply be related to the numbers of latently infected cells.

KSHV-positive cells during the early stage of KS. According to the results of quantitative PCR, relatively high numbers of KSHV copies were detected in patch-stage KS tissue samples (figure 1*D*). In addition, KSHV-positive cells were detected at a rate of ~50% even during the early stage of KS, although numbers of viral copies in DNA from patch-stage samples were lower than those in nodular-stage samples. To clarify why such a high number of viral copies was present during the patch stage of KS, we investigated the localization of KSHV-positive cells in histologically stained sections at the patch stage. Histologic analysis showed an abnormal enlargement of blood capillaries with extended endothelial cells during the patch stage (figure 4*A*). Spindle cells were also sometimes observed around vessels at this stage. Many previous research groups have reported that these spindle-shaped cells were positive for KSHV; however, there has been no report that has described the KSHV status of these extended endothelial cells in enlarged capillaries during the early stage of KS. Here, double labeling revealed that both enlarged endothelial cells and spindle cells around capillaries were positive for LANA and VEGFR-3 (figure 4*A* and 4*B*). VEGFR-3 is a marker of lymphatic endothelial cells, and it is known that KSHV infection alters the gene profile and induces the expression of VEGFR-3 in endothelial cells [31–33]. All KS spindle cells at every stage expressed both LANA and VEGFR-3 (figure 4*A*–4*F*). No signal for LANA or VEGFR-3 was found in normal endothelial cells from capillaries or blood vessels in KS lesions (figure 4*C* and 4*D*). These data suggest that KSHV may infect endothelial cells at a very early

Figure 4. Kaposi sarcoma (KS)–associated herpesvirus–positive cells in various stages of KS. *A* and *B*, hematoxylin-eosin (HE) staining *(A)* and double immunohistochemical staining *(B)* of vascular endothelial cell growth factor receptor 3 (VEGFR-3) *(blue)* and latency-associated nuclear antigen (LANA) *(brown)* in serial sections of patch-stage KS. Original magnification, ×400. *C* and *D*, HE staining *(C)* and double immunohistochemical analysis *(D)* of VEGFR-3 *(blue)* and LANA *(red)* in serial sections of plaque-stage KS. Arrowheads indicate vascular endothelial cells. Original magnification, ×400. *E* and *F*, Double immunohistochemical analysis of VEGFR-3 *(blue)* and LANA *(red)* in nodular-stage KS. Original magnifications, ×100 *(E)* and ×400 *(F)*.

stage in KS lesions and that infection may induce an abnormal extension of endothelial cells and an enlargement of blood vessels, resulting in a relatively high number of KSHV copies.

DISCUSSION

In the present study, we evaluated numbers of viral copies and numbers of KSHV-infected cells in KSHV-associated diseases using real-time quantitative PCR and a computerized-image analytical method. The predicted number of KSHV copies was 3.2 viral copies/cell. The expression of ORF50 protein was rare or nonexistent in KS lesions, which suggests that latently infected cells were proliferating in KS lesions. In MCD samples, 25% of KSHV-infected cells expressed ORF50 protein, which implies that the lytic replication of KSHV was frequent in MCD lesions. To our knowledge, this is the first study describing both numbers of viral copies and numbers of virus-infected cells in pathologic samples from KSHV-associated disease lesions.

The combination of real-time PCR and computerized-image analysis allowed the prediction of numbers of viral copies per infected cell in each KSHV-associated disease. Predicted copy numbers per infected cell are listed in table 3. KS lesions might contain 0.27–5.89 viral copies/cell (average, 3.22 viral copies/cell) of KSHV. KSHV-associated solid lymphoma cells might contain >10 viral copies/cell. These numbers were close to the ones reported for KS cells (1 viral copy/cell) and PEL cells (50 viral copies/cell) [18, 19]. Because almost all KS cells express

LANA, a KS cell should have >1 copy of the virus. One molecule of LANA binds to 1 copy of the KSHV genome on chromosomes of host cells [34]. Immunohistochemical staining produces several dots of LANA in the nucleus of every KS cell [4, 6]. Thus, it is not surprising that a KS cell has several copies of KSHV. Like KS cells, PEL and KSHV-associated solid lymphoma cells exhibited several dots of LANA staining in their nucleus by immunohistochemical analysis, which suggests that PEL and KSHV-associated solid lymphoma cells also have several copies per cell. However, numbers of viral copies in PEL and KSHV-associated solid lymphoma cells were obviously higher than those in KS cells. One reason for that was that 3% of KSHV-associated solid lymphoma cells expressed ORF50 protein, which implies that a small population of lymphoma cells was in the lytic phase, whereas cells expressing ORF50 protein were very rare (<0.1%) in KS cells (table 3). These data suggest that there might be different systems involved in the maintenance or replication of viruses between KSHV-infected lymphoma cells and KS cells. KSHV-positive cells contained 3.38 viral copies/cell in MCD. This number seemed to be lower than what we expected, given that one-fourth of KSHV-infected cells expressed ORF50 protein. We could not determine numbers of viral copies in MCD, because numbers of viral copies might vary among cases, and we examined the virus titer in only one MCD sample. Further studies are definitely required to determine numbers of viral copies in MCD.

Our double immunohistochemical analysis revealed that flat endothelial cells of atypical vessels in early KS lesions expressed both LANA and VEGFR-3. It was difficult to distinguish KS cells from non-KS endothelial cells strictly in HE-stained sections of early KS lesions. VEGFR-3 is a useful marker for KS cells [33]. Our data suggest that a large proportion of extended endothelial cells in the patch stage of KS and KS spindle cells were already infected with KSHV. Because lytic protein expression was also rare during the patch stage, KSHV infected these cells latently. Thus, KSHV infection may be established in endothelial cells at a very early stage in KS lesions. We suggest that this is one of the reasons why numbers of KSHV copies in patch-stage lesions were similar to those in nodular-stage lesions of classic KS in real-time PCR results (figure 3).

Computerized-image analysis has been used by several groups to count cells in immunohistochemically stained sections [35–37]. Technically, our image analysis method was much easier than previously reported ones, in that (1) image files did not need to be captured at high magnification—relatively low magnifications (×40–×100, not ×400) are preferred; (2) splitting of images to red, green, and blue and counting of cells were done automatically; (3) tracing positive and negative cells could be easily visually confirmed; (4) it took only a few minutes to analyze an image; and (5) ImageJ is freeware. The unique features of the present study involve the combination of real-time PCR and computerized-image analysis. Real-time PCR is a powerful tool for measuring numbers of viral copies quickly and easily. However, every pathologic sample contains various numbers of normal cells, and it is impossible to extract DNA strictly from lesions in pathologic samples. Therefore, when DNA is extracted from pathologic samples that contain virus-infected cells, extracted DNA will contain not only DNA from virus-infected cells but also DNA from uninfected cells. Almost all studies that use real-time PCR encounter this limitation. Immunohistochemical analysis and in situ hybridization (ISH) are useful techniques that allow the localization of virus-infected cells. However, immunohistochemical analysis and ISH are not quantitative. Indeed, signal intensity does not correlate with copy number of the molecules or nucleotides, because signal intensity in immunohistochemical analysis and ISH differs among experiments and slides and depends on the conditions of staining or hybridization, such as incubation time, washing, temperature, fixation, and buffer. By combining real-time PCR and computerized-image analysis, the determination of relatively accurate virus numbers in infected cells becomes possible. Numbers of viral copies can be measured using real-time PCR, and numbers of virus-infected cells can be estimated with computerized-image analysis. Both results are required to assess numbers of viral copies in a virus-infected cell. In the present study, we analyzed 1 or a few pictures per slide using computerized-image analysis. Examination of a whole slide would be ideal; however, it is difficult to scan a whole slide using a high-resolution objective lens, but that may be available in the near future using, for example, a virtual slide system. In conclusion, the combination of real-time PCR and computerized-image analysis provides a useful tool for the prediction of numbers of viral copies in virus-associated diseases and of numbers of copies of certain molecules in a cell.

References

1. Moore PS, Chang Y. Kaposi's sarcoma-associated herpesvirus. In: Knipe DM, Howley PM, eds. Fields virology. Vol 2, 4th ed. Philadelphia: Lippincott, Williams & Wilkins, **2001**:2803–33.
2. Moore PS, Chang Y. Detection of herpesvirus-like DNA sequences in Kaposi's sarcoma in patients with and without HIV infection. N Engl J Med **1995**; 332:1181–5.
3. Dupin N, Grandadam M, Calvez V, et al. Herpesvirus-like DNA sequences in patients with Mediterranean Kaposi's sarcoma. Lancet **1995**; 345:761–2.
4. Katano H, Sato Y, Kurata T, Mori S, Sata T. High expression of HHV-8-encoded ORF73 protein in spindle-shaped cells of Kaposi's sarcoma. Am J Pathol **1999**; 155:47–52.
5. Dupin N, Fisher C, Kellam P, et al. Distribution of human herpesvirus-8 latently infected cells in Kaposi's sarcoma, multicentric Castleman's disease, and primary effusion lymphoma. Proc Natl Acad Sci USA **1999**; 96:4546–51.
6. Parravicini C, Chandran B, Corbellino M, et al. Differential viral protein expression in Kaposi's sarcoma-associated herpesvirus-infected diseases: Kaposi's sarcoma, primary effusion lymphoma, and multicentric Castleman's disease. Am J Pathol **2000**; 156:743–9.
7. Nador RG, Cesarman E, Chadburn A, et al. Primary effusion lym-

phoma: a distinct clinicopathologic entity associated with the Kaposi's sarcoma-associated herpes virus. Blood **1996**; 88:645–56.
8. Katano H, Suda T, Morishita Y, et al. Human herpesvirus 8-associated solid lymphomas that occur in AIDS patients take anaplastic large cell morphology. Mod Pathol **2000**; 13:77–85.
9. Chadburn A, Hyjek E, Mathew S, Cesarman E, Said J, Knowles DM. KSHV-positive solid lymphomas represent an extra-cavitary variant of primary effusion lymphoma. Am J Surg Pathol **2004**; 28:1401–16.
10. Soulier J, Grollet L, Oksenhendler E, et al. Kaposi's sarcoma-associated herpesvirus-like DNA sequences in multicentric Castleman's disease. Blood **1995**; 86:1276–80.
11. Suda T, Katano H, Delsol G, et al. HHV-8 infection status of AIDS-unrelated and AIDS-associated multicentric Castleman's disease. Pathol Int **2001**; 51:671–9.
12. Sun R, Lin SF, Staskus K, et al. Kinetics of Kaposi's sarcoma-associated herpesvirus gene expression. J Virol **1999**; 73:2232–42.
13. Rivas C, Thlick AE, Parravicini C, Moore PS, Chang Y. Kaposi's sarcoma-associated herpesvirus LANA2 is a B-cell-specific latent viral protein that inhibits p53. J Virol **2001**; 75:429–38.
14. Rainbow L, Platt GM, Simpson GR, et al. The 222- to 234-kilodalton latent nuclear protein (LNA) of Kaposi's sarcoma-associated herpesvirus (human herpesvirus 8) is encoded by orf73 and is a component of the latency-associated nuclear antigen. J Virol **1997**; 71:5915–21.
15. Lukac DM, Kirshner JR, Ganem D. Transcriptional activation by the product of open reading frame 50 of Kaposi's sarcoma-associated herpesvirus is required for lytic viral reactivation in B cells. J Virol **1999**; 73: 9348–61.
16. Zhu FX, Cusano T, Yuan Y. Identification of the immediate-early transcripts of Kaposi's sarcoma-associated herpesvirus. J Virol **1999**; 73: 5556–67.
17. Katano H, Sato Y, Kurata T, Mori S, Sata T. Expression and localization of human herpesvirus 8-encoded proteins in primary effusion lymphoma, Kaposi's sarcoma, and multicentric Castleman's disease. Virology **2000**; 269:335–44.
18. Cesarman E, Chang Y, Moore PS, Said JW, Knowles DM. Kaposi's sarcoma-associated herpesvirus-like DNA sequences in AIDS-related body-cavity-based lymphomas. N Engl J Med **1995**; 332:1186–91.
19. Lallemand F, Desire N, Rozenbaum W, Nicolas JC, Marechal V. Quantitative analysis of human herpesvirus 8 viral load using a real-time PCR assay. J Clin Microbiol **2000**; 38:1404–8.
20. White IE, Campbell TB. Quantitation of cell-free and cell-associated Kaposi's sarcoma-associated herpesvirus DNA by real-time PCR. J Clin Microbiol **2000**; 38:1992–5.
21. Campbell TB, Borok M, Gwanzura L, et al. Relationship of human herpesvirus 8 peripheral blood virus load and Kaposi's sarcoma clinical stage. AIDS **2000**; 14:2109–16.
22. Tedeschi R, Enbom M, Bidoli E, Linde A, De Paoli P, Dillner J. Viral load of human herpesvirus 8 in peripheral blood of human immunodeficiency virus-infected patients with Kaposi's sarcoma. J Clin Microbiol **2001**; 39:4269–73.
23. Quinlivan EB, Zhang C, Stewart PW, Komoltri C, Davis MG, Wehbie RS. Elevated virus loads of Kaposi's sarcoma–associated human herpesvirus 8 predict Kaposi's sarcoma disease progression, but elevated levels of human immunodeficiency virus type 1 do not. J Infect Dis **2002**; 185:1736–44.
24. Boivin G, Cote S, Cloutier N, Abed Y, Maguigad M, Routy JP. Quantification of human herpesvirus 8 by real-time PCR in blood fractions of AIDS patients with Kaposi's sarcoma and multicentric Castleman's disease. J Med Virol **2002**; 68:399–403.
25. Engels EA, Biggar RJ, Marshall VA, et al. Detection and quantification of Kaposi's sarcoma-associated herpesvirus to predict AIDS-associated Kaposi's sarcoma. AIDS **2003**; 17:1847–51.
26. Song J, Yoshida A, Yamamoto Y, et al. Viral load of human herpesvirus 8 (HHV-8) in the circulatory blood cells correlates with clinical progression in a patient with HHV-8-associated solid lymphoma with AIDS-associated Kaposi's sarcoma. Leuk Lymphoma **2004**; 45:2343–7.
27. Renne R, Zhong W, Herndier B, et al. Lytic growth of Kaposi's sarcoma-associated herpesvirus (human herpesvirus 8) in culture. Nat Med **1996**; 2:342–6.
28. Katano H, Hoshino Y, Morishita Y, et al. Establishing and characterizing a CD30-positive cell line harboring HHV-8 from a primary effusion lymphoma. J Med Virol **1999**; 58:394–401.
29. Chang Y, Cesarman E, Pessin MS, et al. Identification of herpesvirus-like DNA sequences in AIDS-associated Kaposi's sarcoma. Science **1994**; 266:1865–9.
30. Katano H, Sato Y, Itoh H, Sata T. Expression of human herpesvirus 8 (HHV-8)-encoded immediate early protein, open reading frame 50, in HHV-8-associated diseases. J Hum Virol **2001**; 4:96–102.
31. Hong YK, Foreman K, Shin JW, et al. Lymphatic reprogramming of blood vascular endothelium by Kaposi sarcoma-associated herpesvirus. Nat Genet **2004**; 36:683–5.
32. Wang HW, Trotter MW, Lagos D, et al. Kaposi sarcoma herpesvirus-induced cellular reprogramming contributes to the lymphatic endothelial gene expression in Kaposi sarcoma. Nat Genet **2004**; 36:687–93.
33. Weninger W, Partanen TA, Breiteneder-Geleff S, et al. Expression of vascular endothelial growth factor receptor-3 and podoplanin suggests a lymphatic endothelial cell origin of Kaposi's sarcoma tumor cells. Lab Invest **1999**; 79:243–51.
34. Ballestas ME, Chatis PA, Kaye KM. Efficient persistence of extrachromosomal KSHV DNA mediated by latency-associated nuclear antigen. Science **1999**; 284:641–4.
35. Chantrain CF, DeClerck YA, Groshen S, McNamara G. Computerized quantification of tissue vascularization using high-resolution slide scanning of whole tumor sections. J Histochem Cytochem **2003**; 51:151–8.
36. Johansson AC, Visse E, Widegren B, Sjogren HO, Siesjo P. Computerized image analysis as a tool to quantify infiltrating leukocytes: a comparison between high- and low-magnification images. J Histochem Cytochem **2001**; 49:1073–79.
37. Lehr HA, Mankoff DA, Corwin D, Santeusanio G, Gown AM. Application of photoshop-based image analysis to quantification of hormone receptor expression in breast cancer. J Histochem Cytochem **1997**; 45: 1559–65.

References

1. Forastiere F, Stafoggia M, Picciotto S, Bellander T, D'Ippoliti D, Lanki T, von Klot S, Nyberg F, Paatero P, Peters A, *et al.* A case-crossover analysis of out-of-hospital coronary deaths and air pollution in Rome, Italy. *Am J Respir Crit Care Med* 2005;172:1549–1555.
2. Schwartz J, Park SK, O'Neill MS, Vokonas PS, Sparrow D, Weiss S, Kelsey K. Glutathione-S-transferase M1, obesity, statins, and autonomic effects of particles: gene-by-drug-by-environment interaction. *Am J Respir Crit Care Med* 2005;172:1529–1533.
3. Romieu I, Téllez-Rojo MM, Lazo M, Manzano-Patiño A, Cortez-Lugo M, Julian P, Bélanger MC, Hernandez-Avila M, Holguin F. Omega-3 fatty acid prevents heart rate variability reductions associated with particulate matter. *Am J Respir Crit Care Med* 2005;172:1534–1540.
4. Cascio WE. Cardiopulmonary health effects of air pollution: is a mechanism emerging? *Am J Respir Crit Care Med* 2005;172:1482–1484.
5. Brunekreef B, Holgate ST. Air pollution and health. *Lancet* 2002;360:1233–1242.
6. Pope CA III, Burnett RT, Thurston GD, Manzano-Patiño A, Cortez-Lugo M, Julien P, Bélanger MC, Hernandez-Avila M, Holguin F. Cardiovascular mortality and long-term exposure to particulate air pollution. Epidemiological evidence of general pathophysiological pathways of disease. *Circulation* 2004;109:71–77.
7. Brook RD, Franklin B, Cascio W, Hong Y, Howard G, Lipsett M, Luepker R, Mittleman M, Samet J, Smith SC Jr, *et al.* Air pollution and cardiovascular disease: a statement for healthcare professionals from the Expert Panel on Population and Prevention Science of the American Heart Association. *Circulation* 2004;109:2655–2671.

DOI: 10.1164/rccm.2508005

Herpesvirus-associated Pulmonary Hypertension?

Herpesviruses have brilliantly adapted to survive in their host of choice, employing specialized gene products that facilitate their transmission, replication (through cell lysis), and persistence (through latency). Unfortunately, the actions of many of these viral gene products negatively impact infected cells (1), ultimately leading to malignancies and lymphoproliferative diseases, particularly in immunodeficient individuals (2). In 1994, a novel γ herpesvirus homologous to Epstein-Barr virus was detected in Kaposi's sarcoma (KS) lesions from patients with AIDS, and was named Kaposi's sarcoma–associated herpesvirus (KSHV or human herpesvirus 8, HHV-8) (3). This initial finding immediately sparked an intense investigation into the manner in which a herpesvirus could trigger this neoplasm, which was composed of transformed spindle cells with potent angioproliferative properties. The causal role of KSHV has also been established in other malignancies, such as primary effusion lymphoma, and in benign diseases, such as multicentric Castleman's disease, a lymphadenopathy with polyclonal hypergammaglobulinemia (4).

In 2003, Cool and colleagues demonstrated the presence of KSHV in primary pulmonary hypertension (PPH), a disease of the pulmonary arterial wall that is histologically characterized by a lumen-occluding vascular or plexiform lesion containing endothelial and smooth muscle cells (5). Clinically, PPH is characterized by an elevation in pulmonary arterial pressure and eventual heart failure. Although genetic mutations in bone morphogenic protein receptor 2 have been detected in familial cases of PPH (6), no other genetic mutation had been uniformly detected in PPH, leading these investigators to speculate that an infectious agent, plausibly KSHV, may play a causative role in PPH. Their evidence for KSHV infection in PPH stemmed from an initial screen of laser-capture microdissected (LCM) plexiform lesions in which they detected open reading frame (ORF) 26 from KSHV in 4 of 15 patients. Further polymerase chain reaction (PCR) and immunohistochemical analysis by this group revealed the presence of KSHV genome (v-cyclin encoded by ORF72) and KSHV-encoded latency-associated nuclear antigen-1 (LANA-1), respectively, in plexiform lesions and cells outside these lesions (5). However, these results generated immediate controversy as Henke-Gendo and colleagues (7) reported that KSHV infectivity (based on plasma seropositivity) did not differ between the PPH and healthy control groups they studied. Cool and colleagues (7) countered with previously published data showing that nearly 20% of serum samples are negative in patients with KS. However, three independent research groups, using sophisticated immunohistochemical and PCR techniques, have subsequently failed to consistently show the presence of KSHV in PPH lung lesions (8–10). In this issue of the *Journal* (pp. 1581–1585) Henke-Gendo and colleagues (11) call into further question whether KSHV is associated with PPH since their sensitive PCR techniques failed to detect KSHV genome in formalin-fixed lung sections despite evidence of LANA-1 positivity in approximately 62% of these samples.

Conflicting results are common in biomedical research, and differential findings are often simplistically explained by sampling and/or analysis differences. Nevertheless, detection of KSHV genome and protein products is complicated by a number of technical issues relating to the complex lytic and latent phases of this herpesvirus, the status of the tissue analyzed (i.e., fresh vs. fixed; LCM plexiform lesions vs. whole tissues), and the relative abundance of KSHV-infected cells in the analyzed tissue. Immunohistochemical localization of LANA-1 has proven to be a reliable diagnostic tool in screening for the presence of KSHV in KS lesions. The KSHV genome has been detected by PCR in various diseases, including multiple myeloma, Bowen disease, sarcoidosis, and idiopathic pulmonary fibrosis, but LANA-1 staining in tissues associated with these diseases has proven to be elusive, leading many to question the presence and role of KSHV in each (2). Surprisingly, both Cool and coworkers (5) and Henke-Gendo and colleagues (11) showed strong LANA-1 staining in PPH lesions. In both studies, the LANA-1 staining observed in PPH plexiform lesions was suggestive of the "speckled" nuclear pattern classically observed in KS lesions. However, Henke-Gendo and colleagues (11) conclude that the LANA-1 staining they observed was a false-positive finding since they failed to detect KSHV genome by PCR in their lung samples.

Although the bulk of the published data now indicates that it very unlikely that KSHV is present in PPH, it is too soon to rule out the presence of and a putative role for other herpesviruses (or some yet-to-be-discovered virus) in PPH for several reasons. First, there is a striking similarity between the plexiform lesions observed in PPH and cutaneous KS; both exhibit slitlike vascular spaces with sheets of endothelial cells expressing factor 8–related antigen and vascular endothelial growth factor. Second, PPH is a heterogeneous disease, which involves a complex interplay of several genetic and environmental factors. Third, the murine viral equivalent of KSHV has been shown to profoundly remodel the lung (12, 13). Finally, novel antiviral approaches may be in order for the treatment of PPH given the beneficial effects of valacyclovir in idiopathic pulmonary fibrosis (14) and sirolimus in renal-transplant recipients (15). At the very least, clarification of the presence of KSHV in PPH will benefit from the implementation of novel genomic and proteomic detection techniques to LCM plexiform lesions.

Conflict of Interest Statement: Neither of the authors has a financial relationship with a commercial entity that has an interest in the subject of this manuscript.

HARUTAKA KATANO, D.D.S.
National Institute of Infectious Diseases
Tokyo, Japan

CORY M. HOGABOAM, PH.D.
University of Michigan Medical School
Ann Arbor, Michigan

References

1. Hong YK, Foreman K, Shin JW, Hirakawa S, Curry CL, Sage DR, Libermann T, Dezube BJ, Fingeroth JD, Detmar M. Lymphatic reprogramming of blood vascular endothelium by Kaposi sarcoma-associated herpesvirus. *Nat Genet* 2004;36:683–685.
2. Moore PS, Chang Y. Kaposi's sarcoma-associated herpesvirus. In: Knipe DM, Howley PM, editors. Fields virology. 4th ed. Philadelphia: Lippincott, Williams, & Wilkins; 2001.
3. Chang Y, Cesarman E, Pessin MS, Lee F, Culpepper J, Knowles DM, Moore PS. Identification of herpesvirus-like DNA sequences in AIDS-associated Kaposi's sarcoma. *Science* 1994;266:1865–1869.
4. Katano H, Sato Y, Kurata T, Mori S, Sata T. Expression and localization of human herpesvirus 8-encoded proteins in primary effusion lymphoma, Kaposi's sarcoma, and multicentric Castleman's disease. *Virology* 2000;269:335–344.
5. Cool CD, Rai PR, Yeager ME, Hernandez-Saavedra D, Serls AE, Bull TM, Geraci MW, Brown KK, Routes JM, Tuder RM, *et al.* Expression of human herpesvirus 8 in primary pulmonary hypertension. *N Engl J Med* 2003;349:1113–1122.
6. Deng Z, Morse JH, Slager SL, Cuervo N, Moore KJ, Venetos G, Kalachikov S, Cayanis E, Fischer SG, Barst RJ, *et al.* Familial primary pulmonary hypertension (gene PPH1) is caused by mutations in the bone morphogenetic protein receptor-II gene. *Am J Hum Genet* 2000;67:737–744.
7. Henke-Gendo C, Schulz TF, Hoeper MM. HHV-8 in pulmonary hypertension. *N Engl J Med* 2004;350(2):194–195; author reply 195.
8. Laney AS, De Marco T, Peters JS, Malloy M, Teehankee C, Moore PS, Chang Y. Kaposi sarcoma-associated herpesvirus and primary and secondary pulmonary hypertension. *Chest* 2005;127:762–767.
9. Katano H, Ito K, Shibuya K, Saji T, Sato Y, Sata T. Lack of human herpesvirus 8 infection in lungs of Japanese patients with primary pulmonary hypertension. *J Infect Dis* 2005;191:743–745.
10. Daibata M, Miyoshi I, Taguchi H, Matsubara H, Date H, Shimizu N, Ohtsuki Y. Absence of human herpesvirus 8 in lung tissues from Japanese patients with primary pulmonary hypertension. *Respir Med* 2004;98:1231–1232.
11. Henke-Gendo C, Mengel M, Hoeper MM, Alkharsah K, Schulz TF. Absence of Kaposi's sarcoma-associated herpesvirus in patients with pulmonary arterial hypertension. *Am J Respir Crit Care Med* 2005;172:1581–1585.
12. Lok SS, Haider Y, Howell D, Stewart JP, Hasleton PS, Egan JJ. Murine gammaherpes virus as a cofactor in the development of pulmonary fibrosis in bleomycin resistant mice. *Eur Respir J* 2002;20:1228–1232.
13. Dunne DW, Butterworth AE, Fulford AJ, Kariuki HC, Langley JG, Ouma JH, Capron A, Pierce RJ, Sturrock RF. Immunity after treatment of human schistosomiasis: association between IgE antibodies to adult worm antigens and resistance to reinfection. *Eur J Immunol* 1992;22:1483–1494.
14. Tang YW, Johnson JE, Browning PJ, Cruz-Gervis RA, Davis A, Graham BS, Brigham KL, Oates JA Jr, Loyd JE, Stecenko AA. Herpesvirus DNA is consistently detected in lungs of patients with idiopathic pulmonary fibrosis. *J Clin Microbiol* 2003;41:2633–2640.
15. Stallone G, Schena A, Infante B, Di Paolo S, Loverre A, Maggio G, Ranieri E, Gesualdo L, Schena FP, Grandaliano G. Sirolimus for Kaposi's sarcoma in renal-transplant recipients. *N Engl J Med* 2005;352:1317–1323.

DOI: 10.1164/rccm.2509008

研究成果の刊行に関する一覧表

1．書籍

該当なし

2．雑誌

発表者氏名	論文タイトル名	発表誌名	巻号	ページ	出版年
Tomonari A, Takahashi S, Shimohakamada Y, Ooi J, Takasugi K, Ohno N, Konuma T, Uchimaru K, Tojo A, Odawara T, Nakamura T, Iwamoto A, Asano S.	Unrelated cord blood transplantation for a human immunodeficiency virus-1-seropositive patient with acute lymphoblastic leukemia.	Bone Marrow Transplant	36	261-262	2005
T. Maeda, T. Fujii, T. Matsumura, T. Endo, T. Odawara, D. Itoh, Y Inoue, T. Okubo, A. Iwamoto, T. Nakamura.	AIDS-related cerebral toxoplasmosis with hypertense foci on T1-weighted MR images: A case report.	J. Infect.	in press		

Bone Marrow Transplantation (2005) 36, 261–262

www.nature.com/bmt

Correspondence

Unrelated cord blood transplantation for a human immunodeficiency virus-1-seropositive patient with acute lymphoblastic leukemia

Bone Marrow Transplantation (2005) **36**, 261–262. doi:10.1038/sj.bmt.1705028; published online 23 May 2005

The concurrent use of highly active antiretroviral therapy (HAART) improves results of high-dose chemotherapy with autologous stem cell transplantation (SCT) for human immunodeficiency virus-1 (HIV)-associated lymphomas.[1] Recently, successful allogeneic SCT from HLA-matched sibling donors was reported in HIV-infected patients.[2–4] Here, we describe the first case of an HIV-infected patient with acute lymphoblastic leukemia (ALL) who underwent umbilical cord blood transplantation (CBT).

In July 1996, a 23-year-old Japanese woman presented with fever and genital herpes. She was confirmed as seropositive for HIV, probably transmitted from her boyfriend. In March 2001, a real-time quantitative polymerase chain reaction (PCR) analysis showed that the HIV-RNA level was elevated to 25 000 copies/ml (lower limit of detection, 50). The CD4 count decreased to 28/μl. Therefore, HAART consisting of 60 mg stavudine, 300 mg lamivudine, and 600 mg efavirenz was initiated. In July 2001, the HIV-RNA level decreased to 220 copies/ml, and the CD4 count increased to 129/μl. In May 2003, her complete blood count tests showed a white blood cell count (WBC) of 3990/μl with 29% lymphoblasts. Bone marrow (BM) examination showed hypercellularity with 96% lymphoblasts, which were positive for CD4, CD10, CD13, CD19, CD33, CD34, and HLA-DR. Cytogenetic analysis disclosed the presence of t(9;22)(q34;q11) in 12 of 20 metaphases. The p190$^{BCR-ABL}$ transcript was shown by a reverse transcriptase (RT)-PCR analysis. She was diagnosed as Philadelphia chromosome-positive ALL. She achieved hematological complete remission after two courses of chemotherapy. She has been taking HAART during and after the chemotherapy and her HIV-RNA level continued to be below detectable levels. She was negative for hepatitis B virus surface antigen and anti-hepatitis C virus antibody, and positive for anti-cytomegalovirus antibody. As she had no HLA-matched related or unrelated BM donors, the patient underwent CBT from an unrelated donor with mismatches at two loci (HLA-B and DR) in September 2003 (Figure 1). The numbers of total nucleated cells and CD34-positive cells in the cord

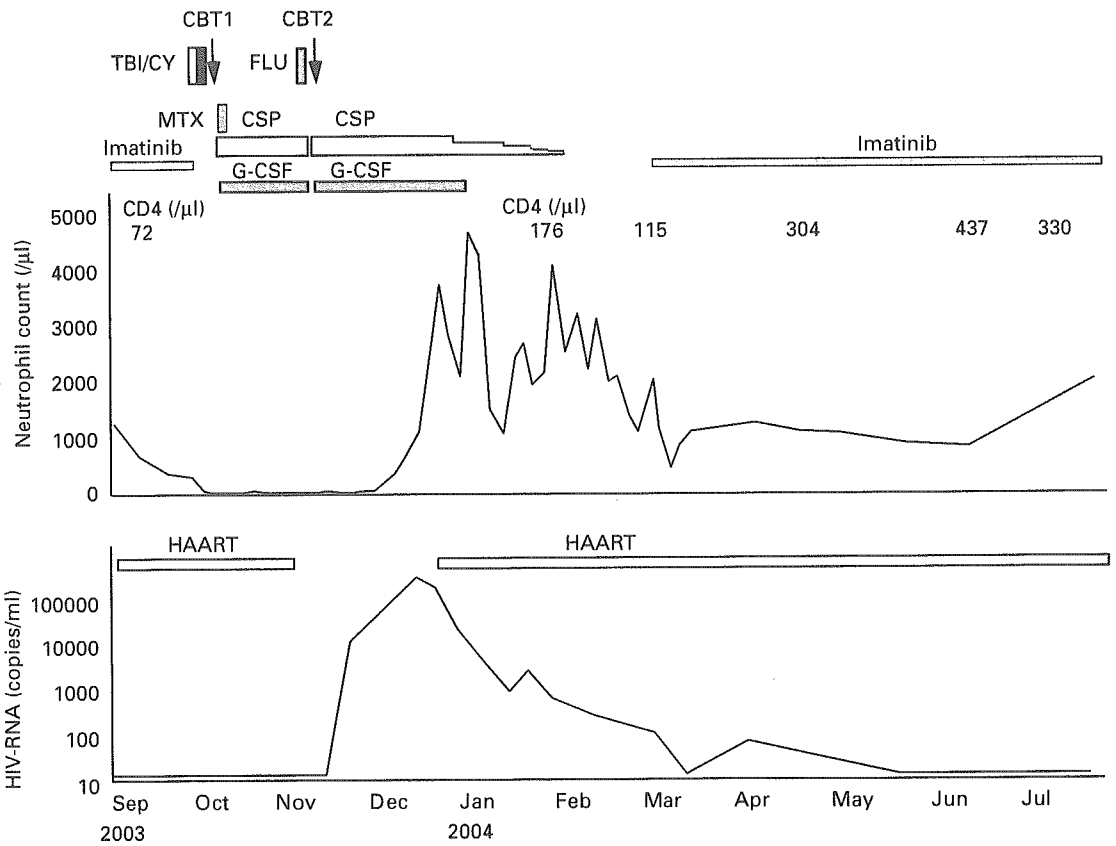

Figure 1 Clinical course of the patient.

blood (CB) unit were 2.9×10^7/kg and 0.76×10^5/kg, respectively. The conditioning regimen included 12 Gy total body irradiation and 120 mg/kg cyclophosphamide. Graft-versus-host disease (GVHD) prophylaxis consisted of cyclosporine and methotrexate. The patient tolerated the procedure well with minimal regimen-related toxicity. Owing to possible myelosuppression, HAART was discontinued on day +28. On day +33, her WBC remained below 100/μl and all of the BM cells were shown to be derived from the recipient. At 40 days after the first CBT, second CBT was performed from an unrelated donor with a one-locus mismatch at HLA-DR. The numbers of total nucleated cells and CD34-positive cells in the CB unit were 2.1×10^7/kg and 0.46×10^5/kg, respectively. The conditioning regimen included 40 mg/m^2 fludarabine for 3 days. Cyclosporine was administered for GVHD prophylaxis. A neutrophil count consistently greater than 500/μl was achieved on day +27. Full donor chimerism of BM cells was shown on day +28. The HIV-RNA level increased to 3×10^6 copies/ml on day +31. After the administration of HAART from day +38, the HIV-RNA levels returned to below detectable levels from day +195, and the CD4 count increased to above 300/μl from day +170. No bacterial or fungal infections were documented during the first and second CBT processes and cytomegalovirus reactivation was successfully treated with ganciclovir and foscarnet. Grade I acute GVHD occurred, but resolved without any additional immunosuppressants. No chronic GVHD was observed. An RT-PCR analysis showed continuous negative test results for the $p190^{BCR\text{-}ABL}$ transcript until the last follow-up evaluation at 15 months post-CBT.

CBT for adults has been associated with a high rate of early transplantation-related mortality (TRM).[5,6] However, our single-institution experience showed a 1-year TRM of 9% and 2-year disease-free survival of 74% in 68 adults after CBT.[7] Both CB donors and the patient in the present study were Japanese. The lesser genetic diversity in a single ethnic population in our studies might be associated with the favorable outcomes of CBT, such as the lower rates of severe acute GVHD. Although our results suggest that CBT is feasible for HIV-infected patients on HAART, the safety and efficacy should be further examined by prospective studies.

A Tomonari[1]
S Takahashi[1]
Y Shimohakamada[1]
J Ooi[1]
K Takasugi[1]
N Ohno[1]
T Konuma[1]
K Uchimaru[1]
A Tojo[1]
T Odawara[2]
T Nakamura[2]
A Iwamoto[2]
S Asano[1]

[1]*Department of Hematology/Oncology, The Institute of Medical Science, The University of Tokyo, Tokyo, Japan; and*
[2]*Department of Infectious Diseases and Applied Immunology, The Institute of Medical Science, The University of Tokyo, Tokyo, Japan*

References

1 Krishnan A, Zaia J, Forman SJ. Should HIV-positive patients with lymphoma be offered stem cell transplants? *Bone Marrow Transplant* 2003; **32**: 741–748.
2 Schlegel P, Beatty P, Halvorsen R, McCune J. Successful allogeneic bone marrow transplant in an HIV-1-positive man with chronic myelogenous leukemia. *J Acquir Immune Defic Syndr* 2000; **24**: 289–290.
3 Sora F, Antinori A, Piccirillo N *et al.* Highly active antiretroviral therapy and allogeneic CD34(+) peripheral blood progenitor cells transplantation in an HIV/HCV coinfected patient with acute myeloid leukemia. *Exp Hematol* 2002; **30**: 279–284.
4 Kang EM, de Witte M, Malech H *et al.* Nonmyeloablative conditioning followed by transplantation of genetically modified HLA-matched peripheral blood progenitor cells for hematologic malignancies in patients with acquired immunodeficiency syndrome. *Blood* 2002; **99**: 698–701.
5 Laughlin MJ, Eapen M, Rubinstein P *et al.* Outcomes after transplantation of cord blood or bone marrow from unrelated donors in adults with leukemia. *N Engl J Med* 2004; **351**: 2265–2275.
6 Rocha V, Labopin M, Sanz G *et al.* Transplants of umbilical-cord blood or bone marrow from unrelated donors in adults with acute leukemia. *N Engl J Med* 2004; **351**: 2276–2285.
7 Takahashi S, Iseki T, Ooi J *et al.* Single institute comparative analysis of unrelated bone marrow transplantation and cord blood transplantation for adult patients with hematological malignancies. *Blood* 2004; **104**: 3813–3820.

Journal of Infection (2006) ■, ■–■

ELSEVIER

BRITISH INFECTION SOCIETY

www.elsevierhealth.com/journals/jinf

CASE REPORT

AIDS-related cerebral toxoplasmosis with hyperintense foci on T1-weighted MR images: A case report

T. Maeda [a,c,*], T. Fujii [b,c], T. Matsumura [b,c], T. Endo [c], T. Odawara [c], D. Itoh [d], Y. Inoue [d], T. Okubo [d], A. Iwamoto [a,b,c], T. Nakamura [c]

[a] *International Research Center for Infectious Diseases, The Institute of Medical Science, The University of Tokyo, 4-6-1 Shirokanedai, Minato-ku, Tokyo 108-8639, Japan*
[b] *Division of Infectious Diseases, Advanced Clinical Research Center, The Institute of Medical Science, The University of Tokyo, 4-6-1 Shirokanedai, Minato-ku, Tokyo 108-8639, Japan*
[c] *Department of Infectious Diseases and Applied Immunology, Research Hospital, The Institute of Medical Science, The University of Tokyo, 4-6-1 Shirokanedai, Minato-ku, Tokyo 108-8639, Japan*
[d] *Department of Radiology, Research Hospital, The Institute of Medical Science, The University of Tokyo, 4-6-1 Shirokanedai, Minato-ku, Tokyo 108-8639, Japan*

Accepted 8 December 2005

KEYWORDS
Toxoplasmosis;
MRI;
AIDS

Summary The neuroradiological findings are helpful for the diagnosis of toxoplasmic encephalitis. The T1 hypersignal intensity foci on brain magnetic resonance (MR) images without contrast enhancement are presented and can be a pathognomonic sign of this disease.

Introduction

Most toxoplasmic encephalitis is opportunistic infection complicated with the acquired immunodeficiency syndrome (AIDS) and immunosuppressive conditions. The diagnosis of this disease is difficult because of the incompetence of the serological examination for the immunocompromised patients.[1] Although the direct detection method for the pathogen by polymerase chain reaction (PCR) using the cerebrospinal fluid (CSF) has high specificity, the sensitivity of this method is insufficient for definitive diagnosis.[2] We, therefore, have to synthetically diagnose with clinical symptoms, signs, laboratory data, neuroradiological images and the response to anti-toxoplasmosis therapy.

We report here our experience of a unique MR imaging finding of toxoplasmic encephalitis in an

* Corresponding author. International Research Center for Infectious Diseases, The Institute of Medical Science, The University of Tokyo, 4-6-1 Shirokanedai, Minato-ku, Tokyo 108-8639, Japan. Tel: +81 3 5449 5338; fax: +81 3 5449 5427.
E-mail address: tmaeda@ims.u-tokyo.ac.jp (T. Maeda).

0163-4453/$30
doi:10.1016/j.jinf.2005.12.006

AIDS patient and emphasize the hyperintense foci on T1-weighted MR images that can be one of the pathognomonic MR images of this disease.

Case report

A 44-year-old man with disturbance of consciousness and respiratory insufficiency was admitted to our hospital in April 2005. His consciousness had been rapidly deteriorated and he developed coma 2–3 days before hospitalization. Serological tests of HIV antibodies and *Toxoplasma gondii* IgG antibody were positive, but the *T. gondii* IgM antibody was not detected. The concentration of HIV RNA in plasma was 120,000 copies/ml and the CD 4 cell count was 8 mm^{-3}. The chest X-ray showed bilateral ground glass shadow and *Pneumocystis jiroveci* (carinii) was detected from bronchoalveolar lavage (BAL) fluid. CSF showed mild elevated protein level of 65 mg/dl and pleocytosis, and the opening pressure was over 300 mmH_2O. No malignant cells or microorganisms were detected. *T. gondii* B1-gene fragment was detected by PCR using CSF, therefore, the diagnosis of an AIDS case with toxoplasmic encephalitis was made.[3]

MRI of the brain showed multiple high intensity lesions on T2-weighted image (Fig. 1a) and the corresponding T1-wighted image showed low intensity lesions. Contrast enhanced T1-weighted images showed multiple nodular and ring enhancement lesions.

The chemotherapy with trimethoprim/sulfamethoxazole (TMP/SMX) was very effective and the patient's consciousness level was improved gradually. *P. jiroveci* pneumonia was also cured. MR imaging after 4 weeks of treatment demonstrated that the multiple nodular lesions on T1 and T2-weighted images had significantly been reduced. After 8 weeks of treatment, the contrast enhanced T1-weighted images showed only residual small lesions without contrast enhancement. Interestingly, the hypersignal intensity foci appeared at bilateral basal ganglia obviously after 2 weeks of treatment on the non-enhanced T1-weighted images (Fig. 1b). Corresponding computed tomography (CT) image did not show hemorrhagic or calcified densities (Fig. 1c). These T1 hypersignal intensity foci regressed gradually along with antitoxoplasmic chemotherapy in proportion to other mass lesions. The T2* (star)-weighted image, which can detect the hemosiderin deposition as hypointensity lesion, operated after 12 weeks of treatment showed no hypointensity at corresponding T1 hypersignal intensity foci on basal ganglia (Fig. 1d).[4] We concluded that the toxoplasmic encephalitis showed the hypersignal intensity foci on T1-weighted MR imaging without hemorrhage or calcification.

Discussion

Toxoplasmic encephalitis progresses rapidly and is life threatening to immunocompromised patients. Therefore, we often have to start the antitoxoplasmosis therapy when this encephalitis is suspected on the neuroradiologic images and laboratory data. Typically, the toxoplasmic encephalitis lesions on MRI studies appear as T2 hypersignal intensity foci and T1 hypo-isosignal intensity foci, and reveal a rim of enhancement surrounding the edema on contrast enhanced T1-weighted images. Nevertheless, even characteristic foci on these MR imagings are not pathognomonic. Since the differential diagnosis of toxoplasmic encephalitis from other infections or CNS lymphoma is difficult, improvement in the diagnostic methods is an urgent necessity.

In our case, the toxoplasmic encephalitis was diagnosed with the highly specific PCR and confirmed by the response to anti-toxoplasmosis therapy. Brain MRI revealed unusual findings, T1 hypersignal intensity foci, accompanied by typical multiple high intense lesions on T2-weighted image during the treatment. These unique MR findings have been reported on only a few cases of non-HIV/AIDS-related toxoplasmic encephalitis. Terada et al.[5] reported a case of toxoplasmic encephalitis after stem cell transplantation with T1 hypersignal intensity foci. Autopsy revealed the disseminated toxoplasmosis, and coagulative necrosis without hemorrhage or calcification was revealed at corresponding T1 hypersignal intensity foci by neuropathological study. In another post-bone marrow transplantation case, inflammatory and vascular changes without hemorrhage appeared to be the cause of iso or hypersignal intensity rings by the stereotactic biopsy of T1 hypersignal intensity foci.[6] On the other hand, Navia et al.[7] demonstrated that the T1 hypersignal intensity foci were cased by coagulative necrosis with lipid-laden macrophages. The pathophysiological and neuroradiological mechanisms to create these MRI findings are far from clear yet. The reason why the T1 hypersignal intensity foci tend to localize in the basal ganglia is not clear either.[5,6]

CNS lymphoma, which is important for the distinction from toxoplasmic encephalitis, shows T1 hypo-isosignal intensity foci and never shows T1 hypersignal intensity foci except subacute

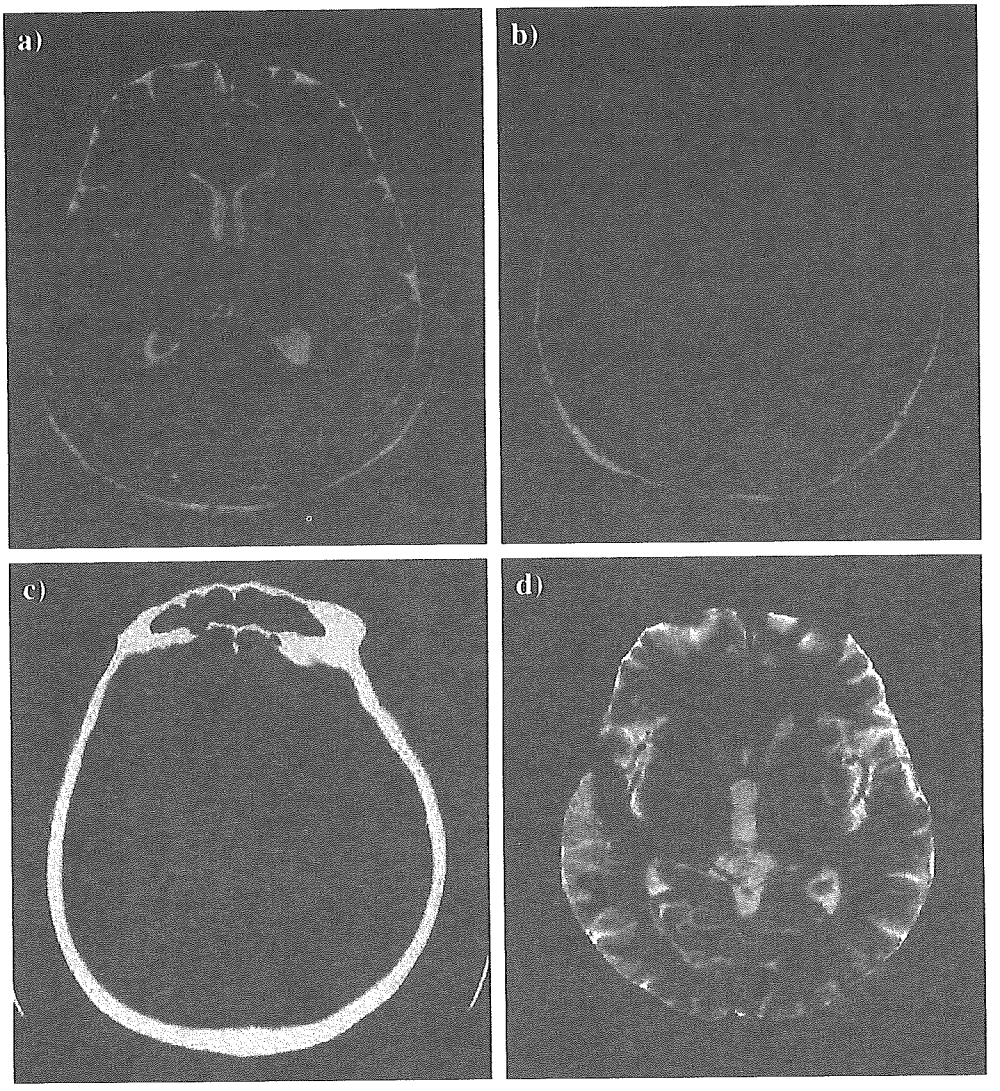

Figure 1 (a) The T2-weighted magnetic resonance image presented multiple high intense lesions. (b) Non-enhanced T1-weighted image showed hypersignal intensity foci at bilateral basal ganglia. (c) The corresponding CT image showed non-hemorrhagic or non-calcified density. (d) The T2* (star)-weighted image showed non-hemorrhagic observations at basal ganglia.

hemorrhage with hypervascular CNS lymphoma.[8,9] However, the CT imaging and T2* (star)-weighted MR imaging can simply distinguish it from the toxoplasmic T1 hypersignal intensity foci without hemorrhage or calcification.

We reported here the unique MRI findings, T1 hypersignal intensity foci, without hemorrhage or calcification on HIV/AIDS-related toxoplasmic encephalitis. It will be helpful for the diagnosis of toxoplasmic encephalitis and may be a pathognomonic finding. Unfortunately, we have not experienced another case of toxoplasmic encephalitis after this case, but we would like to continue to explore this unique MRI finding of this disease.

Acknowledgement

This work was partly supported by the Special Coordination Funds for Promoting Science and Technology of MEXT: strategic cooperation to control emerging and reemerging infections and grants for AIDS research from the Ministry of Health, Labor and Welfare of Japan.

References

1. Luft BJ, Brooks RG, Conley FK, McCabe RE, Remington JS. Toxoplasmic encephalitis in patients with acquired immune deficiency syndrome. *JAMA* 1984;**252**:913–7.

2. Cingolani A, De Luca A, Ammassari A, Murri R, Linzalone A, Grillo R, et al. PCR detection of *Toxoplasma gondii* DNA in CSF for the differential diagnosis of AIDS-related focal brain lesions. *J Med Microbiol* 1996;**45**:472–6.
3. Castro KG, Ward JW, Slutsker L, Buehler JW, Jaffe HW, Ruth L, et al. 1993 revised classification system for HIV infection and expanded surveillance case definition for aids among adolescents and adults. *Morb Mortal Wkly Rep* 1992; **41**:1–19.
4. Bulte JW, Kraitchman DL. Iron oxide MR contrast agents for molecular and cellular imaging. *NMR Biomed* 2004;**17**: 484–99.
5. Terada H, Kamata N, Yokoyama Y, Ohashi K, Akiyama H, Sakamaki H. T1-hypersignal foci in cerebral toxoplasmosis. *Riv Neuroradiol* 2001;**14**:665–7 [Case report].
6. Dietrich U, Maschke M, Dorfler A, Prumbaum M, Forsting M. MRI of intracranial toxoplasmosis after bone marrow transplantation. *Neuroradiology* 2000;**42**:14–8.
7. Navia BA, Petito CK, Gold JW, Cho ES, Jordan BD, Price RW. Cerebral toxoplasmosis complicating the acquired immune deficiency syndrome: clinical and neuropathological findings in 27 patients. *Ann Neurol* 1986;**19**:224–38.
8. Jenkins CN, Colquhoun IR. Characterization of primary intracranial lymphoma by computed tomography: an analysis of 36 cases and a review of the literature with particular reference to calcification haemorrhage and cyst formation. *Clin Radiol* 1998;**53**:428–34 [Review].
9. Rubenstein J, Fischbein N, Aldape K, Burton E, Shuman M. Hemorrhage and VEGF expression in a case of primary CNS lymphoma. *J Neurooncol* 2002;**58**:53–6.